Article:
Mortimer, EJ, Paton, DA, Scholz, CA et al. (2016) Implications of structural inheritance in oblique rift zones for basin compartmentalization: Nkhata Basin, Malawi Rift (EARS). Marine and Petroleum Geology, 72. pp. 110-121. ISSN: 0264-8172

https://doi.org/10.1016/j.marpetgeo.2015.12.018

Implications of structural inheritance in oblique rift zones for basin compartmentalization: Nkhata basin, Malawi Rift (EARS).

Mortimer, E. J.[1], Paton, D. A.[1], Scholz, C. A.[2], Strecker. M. R.[3]

e.j.mortimer@leeds.ac.uk *corresponding author*

[1]Basin Structure Group, School of Earth and Environment, University of Leeds, Leeds, UK.
[2]Department of Earth Sciences, Syracuse University, Syracuse, New York 13244.
[3]Institut f. Geowissenschaften, Universität Potsdam, Postdam, 14476, Germany

Abstract

The Cenozoic East African Rift System (EARS) is an exceptional example of active continental extension, providing opportunities for furthering our understanding of hydrocarbon plays within rifts. It is divided into structurally distinct western and eastern branches. The western branch comprises deep rift basins separated by transfer zones, commonly localised onto pre-existing structures, offering good regional scale hydrocarbon traps. At a basin-scale, local discrete inherited structures might also play an important role on fault localisation and hydrocarbon distribution. Here, we consider the evolution of the Central basin of the Malawi Rift, in particular the influence of pre-existing structural fabrics.

Integrating basin-scale multichannel 2D, and high resolution seismic datasets we constrain the border, Mlowe-Nkhata, fault system (MNF) to the west of the basin and smaller Mbamba fault (MF) to the east and document their evolution. Intra basin structures define a series of horsts, which initiated as convergent transfers, along the basin axis. The horsts are offset along a NE-SW striking transfer fault parallel to and along strike of the onshore Karoo

(Permo-Triassic) Ruhuhu graben. Discrete pre-existing structures probably determined its location and, oriented obliquely to the extension orientation it accommodated predominantly strike-slip deformation, with more slowly accrued dip-slip.

To the north of this transfer fault, the overall basin architecture is asymmetric, thickening to the west throughout; while to the south, an initially symmetric graben architecture became increasingly asymmetric in sediment distribution as strain localised onto the western MNF. The presence of the axial horst increasingly focussed sediment supply to the west. As the transfer fault increased its displacement, so this axial supply was interrupted, effectively starving the south-east while ponding sediments between the western horst margin and the transfer fault. This asymmetric bathymetry and partitioned sedimentation continues to the present-day, overprinting the early basin symmetry and configuration. Sediments deposited earlier become increasingly dissected and fault juxtapositions changed at a small (10-100 m) scale. The observed influence of basin-scale transfer faults on sediment dispersal and fault compartmentalisation due to pre-existing structures oblique to the extension orientation is relevant to analogous exploration settings.

Keywords: East African Rift System; structural inheritance; normal fault evolution; sediment distribution

Introduction

Following the margins of the Tanzanian craton, the East African Rift System (EARS; Figure 1) is divided into two structurally distinct west and east branches (e.g., Ebinger, 1987). Past tectonic activity since the Proterozoic is responsible for inducing structural weakness in the lithosphere, which strongly influences the location and orientation of late-Cenozoic structures in both branches (Rosendahl, 1987; Versfelt and Rosendahl, 1989; Ring et al., 1992). The role of inherited structural fabrics, including PreCambrian mobile belts and Permian Karoo basins is well documented in determining the present-day structural configuration (e.g., Rosendahl, 1987; Versfelt and Rosendahl, 1989; Morley 1990; Morley et al., 1990; Ring et al., 1992; Corti et al., 2007). Comprised of a series of opposing, asymmetric, deep half-graben basins separated by transfer or accommodation zones (Rosendahl, 1987; Ebinger et al., 1984, 1993; Ebinger, 1989) this part of the EARS highlights the potential for hydrocarbon trapping where transfers occur (Morley et al., 1990), and can be likened to those of the Viking graben, North Sea (Scott and Rosendahl, 1989; McLeod et al., 2004).

The Malawi rift (Figure 1) is the southernmost rift of the western branch. The north, Karonga Basin, has undergone oblique extension with a significant component of dextral slip (Chorowicz and Mukonki, 1980; Wheeler and Karson, 1989; Wheeler and Rosendahl, 1994) with a temporal variation in rift obliquity that occurred during the Pleistocene. While initially the region experienced ENE-WSW oriented extension, the changeover to the neotectonic kinematic regime has subjected this region to NW-SE extension (Delvaux et al., 1992; Ring et al., 1992; Scott et al., 1992; Mortimer et al.,

2007). This change in stress orientation occurred c. 500 Ka based upon dated tuffs and the correlation with 100 kyr duration packages in seismic reflection data (Mortimer et al., 2007). This change in orientation is not, however, documented to the west of the basin, where Karonga earthquake focal mechanisms indicate pure extension, and a W-E extension orientation (Biggs et al., 2012). This change in orientation, while influencing the latest stages of basin evolution, appears to have been focussed upon the Mbeya region. Similarly, in the Rukwa basin to the north, stress inversion of earthquakes (Delvaux and Barth, 2010) shows Sh max is NW-SE, invoking an ENE-WSW extension regime today.

Existing models for the development of the western branch focus largely at the rift-scale, with transfer zones that separate basins along the rift providing predictable regions of potentially good hydrocarbon traps (Morley et al., 1990). However, in this study we focus on the basin-scale Cenozoic structural evolution of the c.150 km-long, 40 km-wide central or 'Nkhata' (Ebinger et al., 1987) basin of the Malawi rift which is in part superimposed onto a SW-NE trending Karoo basin preserved onshore and inferred to continue into the region currently occupied by Lake Nyasa (Figure 1). It is bounded to the west by a steep, east-dipping, 120 km border fault system (Mlowe-Nkhata fault) and to the east by a shorter, ~30 km-long, border fault (Mbamba fault; Figure 2a). Utilizing a close-spaced grid of seismic reflection data, we constrain the patterns of fault growth and potential role of existing structural trends, and assess the implications for hydrocarbon prospectivity in this and analogous basins elsewhere.

Data sets, methodology and tectono-stratigraphic framework

Two vintages of seismic reflection data are utilised (Figure 2): (1) 18 basin-scale multi-channel profiles collected by project PROBE, Duke University (Scholz, 1989) recording a maximum of 6 seconds (TWT), incorporate the entire sedimentary fill, and image the top basement reflection; (2) a series of shallow, up to 2 seconds (TWT), seismic reflection data collected in the late 1990s – 2005 that record the recent basin fill (Scholz, 1995). Seismic profiles were interpreted using standard seismic sequence stratigraphic methods (e.g. Mitchum *et al.*, 1977; Hubbard *et al.*, 1985a & b) with Schlumberger Petrel 2D and 3D environments. Interpreted surfaces were gridded (300 m cell size) using standard interpolation methods. The resolution and confidence of fault correlations in map view is a function of line spacing, which, by combining PROBE and shallow surveys, is reduced to ~1.5 - 8 km in the north and centre of the basin. In many instances, therefore, faults have been traced to within 2 km of the fault tip. In the south of the basin, this uncertainty is increased due to greater line spacing. Variation in sediment thickness, generated by subtracting interpolated surfaces, has been used to locate the depocentre for each successive sequence along structures. Depocentre distribution and evolution provide an approximation for the displacement pattern, and thus evolution, of faults (e.g., Schlische and Anders, 1996; McLeod et al., 2000, Contreras et al., 2000; Paton, 2006; Mortimer et al., 2007).

The established tectono-stratigraphic framework of Scholz (1989) for the PROBE sequences, namely: 1A, 1B, 2 and 3 (old to young) is used. Ebinger

et al. (1993) proposed ages for these sequences based upon the presence of dated volcanics and unconformities correlated to unconformities interpreted within the PROBE data that placed the onset of rifting c. 8.6 Ma; Sequence 1-2 boundary at ~ 2.3Ma and the Sequence 2-3 boundary at ~ 1.6 Ma. It is, however, likely that the onset of rifting and sedimentation was considerably earlier than this; with Miocene sediments recorded in the Rukwa Rift to the north (Roberts et al., 2012) and low temperature thermochronology from the Livingstone Mountains (Mortimer et al., 2006) suggesting a Miocene onset c. 20 Ma.

The shallow seismic reflection surveys fit within this tectonostratigraphic context greatly improving the resolution of Sequence 2 and 3, recording the upper 2 seconds TWT. They reveal high frequency cycles that probably correspond to ~100 kyr climatic fluctuations (Scholz, 1995). In the following interpretations, the PROBE data has been used to establish the overall basin geometry, to create the first-order fault model, and to investigate the earliest three stages of basin evolution (Sequences 1A, 1B, and Sequence 2). Within the shallow seismic data, four horizons have been interpreted. The lower three occur within Sequence 2 and the fourth corresponds to PROBE Sequence 3. This integration of the two data sets has led to Sequence 2 being sub-divided into 2A (below the shallow seismic data) and 2B, C, D from oldest to youngest respectively occurring within the shallow seismic data. Sequence 3 has been described using the shallow seismic data in the north and central portions of the basin. To the south, PROBE data has been utilised

in the absence of shallow seismic data. The shallow seismic data has also been utilised to refine the fault model.

Nkhata Basin Setting and Architecture

The Nkhata basin is one of the three deep basins of the Malawi rift that accommodate >4 km sediment, and are connected across transfer, or accommodation, zones (Ebinger, 1987; Versfelt and Rosendahl, 1989; Ebinger et al., 1993). Existing structures of significance are the Ubendian Proterozoic mobile belt, known to have exerted strong influence on the location and orientation of the northern (Karonga) basin of the Malawi Rift (Rosendahl, 1987; King, 1994), and later Permian Karoo extensional basins onto which many basin separating accommodation zones are juxtaposed (e.g., Versfelt and Rosendahl, 1989) . There are significant occurrences of Karoo sediments in a SW-NE graben to the east of the central basin of the Malawi Rift, and some deposits to the west suggesting this graben continues into the region occupied by Lake Nyasa (Figure 1b).

The northern two thirds of the >700 km Malawi Rift is, today, filled by the 700 m deep Lake Nyasa, at its deepest adjacent to the border faults. The Nkhata basin is bounded by the Mlowe-Nkhata Fault (MNF) to the west, the Mbamba Fault to the east, and is dissected by a number of smaller intra-basin faults of varying length and orientation (Figure 2).

The sedimentary fill of the Nkhata basin thickens westward toward the MNF, and thins to the southeast. Where the lake floor is deepest (Figure 2a) is coincident with the thickest sedimentary fill adjacent to the MNF (Figure 2b),

at the centre of this fault. The MNF comprises three border fault segments of 40 km, 60 km, and 40 km length, from north to south respectively (Figure 2). The north and central segments have been recognised by previous interpretations (e.g., Ebinger et al., 1987; Scholz, 1989; Soreghan et al., 1999; Contreras et al., 2000), separated by a relay ramp (Chilumba 'platform' Scholz, 1989) that is dissected by normal, preferentially SW-dipping faults (e.g., Soreghan et al., 1999). The south fault segment was first interpreted by Contreras at al., (2000) based upon PROBE data, however, the greater resolution of our data indicates that it does not continue so far north into the basin as they proposed. The central and south fault segment tips, because of limited data, can only be inferred, but overlap by ~10 km, and are separated by ~6 km.

The geometry of the Nkhata basin varies along axis (Figure 3). To the north (section A-A') it is an asymmetric half-graben with an eastern shoaling margin. Toward the centre (sections B-B' and C-C'), this asymmetry decreases with the development of a more symmetric graben bounded to the west by the east-dipping MNF, and by the west-dipping Mbamba Fault to the east with a horst in the middle of the basin. This horst is offset along strike of the basin, separated into the 'north' and 'central' horsts across Fault 9 (discussed later). The Mbamba Fault is ~30 km and accommodates 1700 ms of sediment in its hanging-wall. Further south in the basin, the prominence of the central horst is reduced (section D-D') and the Mbamba fault to the east is no longer present. Farther south, heading toward the transfer zone into the southern basin of the Malawi Rift, the overall geometry is dominated by thickening of

the sediments into the MNF and the presence of a separate 'southern horst' in the east of the basin (section E-E') that has sediments of Sequence 2 either not deposited or subsequently eroded from its crest.

Within the basin, the architecture is controlled by intra-basin faults with displacements ranging from seismic resolution to a few 100 ms TWT. As it is important to correlate faults across the data, only faults with throws > 100 ms TWT are considered, of which a total of nine (numbered on figures) significant faults are recognised. The majority of the intra-basin faults strike sub-parallel to the MNF, although a small number (faults 9 and 10) have a cross-cutting, NE-SW strike. The basin is divided along its central axis by a series of horsts (Figures 2 and 3), separating a region of considerably greater sedimentation to the west from that in the east (Figure 2b; sections B-B', C-C', E-E' Figure 3). Along their strike the horsts are offset by smaller, cross-cutting faults (e.g., fault 9; Figure 2; section C-C', Figure 3).

Nkhata Basin Evolution

The distribution of depocentres (based upon sediment thickness TWT) for each depositional sequence (Figure 4) has been utilised to reconstruct the spatio-temporal evolution of the basin. Footwall sediments with the exception of minor thicknesses (< 50 ms) are generally not preserved along the MNF; therefore the thickest depocentre is taken to represent the location of maximum displacement (d-max) along the structure. Within the basin, sediment thickness (TWT) variations across structures where footwall sediments are preserved, in addition to the spatio-temporal distribution of depocentres have been used in determining the evolution of intra-basin faults.

Sequence 1A

In the earliest resolvable stages of basin evolution (Figure 4a, Sequence 1A), the MNF comprised four (rather than the present three) individual segments. The north and central MNF segments were separate and it is likely they overlapped. The present-day central segment comprised two segments of similar length (~25 km) that were separated by a high, while the south segment was present but exerted little influence on sedimentation. In the east of the basin, the Mbamba Fault was active along its northern half opposite the high between the two central fault segments.

Within the basin most sedimentation was accommodated across a small population of faults striking sub-parallel to the MNF. Those that exhibit sediment thickening greater than a few hundred ms TWT are Fault 1 (up to 1200 ms TWT) and Fault 5 (>600 ms TWT). These two faults form an opposing half-graben architecture separated by Fault 9 (which has no resolvable dip-displacement at this time); and are antithetic to their border faults the central segments of the MNF (fault 1) and the Mbamba fault (fault 5).

Sequence 1B

In Sequence 1B (Figure 4b) the individual MNF segments each had a depocentre toward their centre, and the Mbamba Fault accommodated as much sediment in its hanging-wall as the MNF fault segments, and along its

entire length. Overall the basin had a striking disparity between the asymmetry in the north, and more symmetric graben to the south. The relay between the north and central fault segments was well established, and sediments are likely to have been transported along this into the hanging-wall adjacent to the north segment fault tip where a significant accumulation is present. The relay represents a high in the basin at this time. Farther south, the central fault segments are still separated by a high.

Within the basin, the total length of the bounding faults of the three horsts was achieved (Figures 4a and b) and a number of 'new' faults within the horsts appear (although they may have been present below seismic resolution prior to this). The northern horst is comprised of four linked faults, two on each margin, with additional smaller faults between them. These also formed with an opposing sense of asymmetry across them (Figures 4a and b). Patterns of sediment distribution along Faults 1 and 2 suggest they had opposing dips and propagated toward one another to develop a horst with fault 2 being a younger structure; similarly Fault 4 (antithetic to fault 5, and bounding the central horst) became active during Sequence 1B. All of Faults 1, 2, 4, and 5 terminate or merge with Fault 9 in the centre of the basin. Fault 4 is antithetic to the now developing central fault segment as displacement moves toward the middle of the basin. Both the north and central horst remain asymmetric across them, and that asymmetric is opposing across Fault 9. The southern horst was present throughout deposition of Sequence 1, dissected by smaller faults in Sequence 1A that were inactive by 1B. Fault 10, in the south of the

basin appears to truncate the southern horst and behave in a similar manner to fault 9, although there is poor data resolution in this portion of the basin.

Sequence 2

During deposition of Sequence 2, the relay between the north and central fault segments was breached (Figure 4c-f) by a number of smaller faults crossing it. The pattern of sedimentation overall within the basin becomes more asymmetric thickening to the west into the MNF, with the intra-basin regions to the east of the horsts experiencing a reduction in sedimentation (aside from the centre of the basin). The total thickness of Sequence 2 (Figure 4c) shows the accumulation of sediment on the relay, the individual packages (Figures 4 d-f) highlight the development of NE-SW trending faults across the relay that at times was bypassed by sediment. It is also during Sequence 2 that the central fault segment depocentres amalgamated from two separate basins (Figure 4d and e) that become progressively closer until they merge (Figure 4f) as the central segment became fully linked overprinting the earlier high. As strain localised onto the MNF, the Mbamba Fault to the east became significantly less important; and the southern MNF segment became more active.

The overall pattern of sedimentation within the basin (Figure 4c), shows that the horsts were established and provided the predominant control on intra-basin sedimentation: that there is little sediment preserved on their footwalls suggests these were regions of non-deposition and possibly emergent highs during lowstand conditions. Overall, the basin is asymmetric with sediments

thinning onto the eastern margin as strain had been localised onto the MNF. Divergent reflections and package thickening indicates significant deposition in the hanging-wall of Fault 1 (at least 600 ms TWT thickening across the fault), Fault 5 (c. 700 ms TWT across it), Fault 2 (c. 600 ms TWT) and Fault 4 (600 ms TWT). Fault 6 was also active, with c. 300 ms TWT thickening across it. Importantly, there is a notable reduction in sediment reaching the south and east of the basin compared to Sequence 1B; additionally, there is an accumulation of sediment in the hanging-wall of Fault 9 and 2 east of the northern horst. The shallow seismic data supplement the PROBE data for the upper portions of Sequence 2 (Figures 4d,e,f) and show the importance of Fault 4, 1, 5 and 9 in the distribution of sediment. Of the three Sequences 2B-D, 2C is likely to represent a period of reduced sediment supply and concentration of sedimentation adjacent to the border fault. During Sequences 2B and C, however, sediments are deposited across the basin, concentrated in the hanging-wall of Fault 4, and Fault 9, with small dissected depocentres developing to the north of Fault 9. To the south east, and into Fault 5, sediments also accumulated, although notably less than to the west, until Sequence 2D, where sedimentation to the south east of Fault 9 is significantly reduced. This coincides with the merging of depocentres on the MNF central segment, and with increased displacement on Fault 9.

Sequence 3

During Sequence 3 (Figure 4g) the southern segment accommodates similar sediment volumes to the central segment, from which it is separated by a probable relay zone, although the absence of high resolution seismic

coverage in this region means it cannot be resolved. By the end of Sequence 2 and during Sequence 3, sedimentation was concentrated adjacent to the central portion of the MNF (Figures 4f and g).

The pattern of sediment distribution within the basin observed for Sequence 2 continues into Sequence 3, where, while the principal structures remain active (e.g., Faults 5, 2) sediment is focussed adjacent to Faults 1, 9, and 4 within the basin and along the central MNF fault segment, and to the north of the basin to a lesser degree. These regions of sediment accommodation are separated by condensed sections which, where they are pronounced, are probably also related to a reduction in the lake dimensions; however, depocentres' location is structurally controlled. Sediment entering the basin to the North deposit a delta fan; while those to the west are likely to comprise both material transported through the relay and some axial transport into the main depocentre, which exhibits a rapid thickening. In this manner while the north of the basin has always been asymmetric throughout its history, the centre of the basin was initially more symmetric with border faults on both west and east, but became increasingly asymmetric in terms of basin-fill as strain localised onto the MNF (Figures 4c and d), and it is this latter asymmetry that is reflected in the present day bathymetry (Figure 2a).

Fault 9

Of the NE-SW striking fault population, Fault 9 (Figure 4) is the best imaged. In cross section (Figure 5a, Section F-F') it has a flower geometry, with a number of smaller dissecting faults affecting the sediments adjacent to it.

Fault 9 exhibits no measurable thickening across it during Sequences 1A and B (Figure 4a and b; PROBE section C-C' Figure 2); however, it is likely to have been present as a transfer fault given the opposing sense of dip between Faults 5 and 1 offset across it. During Sequence 2, a measurable dip-displacement component to Fault 9 becomes apparent, as its footwall is uplifted to the southeast during Sequence 2D (Figure 4f; Figure 5a) and sediment accumulates in its hanging-wall both to the west and east of the northern horst; and to the west of the central horst. Initially, Fault 9 separated two opposing half graben, later antithetic faults developed and it separated the horsts while extension continued. Initially, Fault 1 to the north and Fault 4 to the south of Fault 9 (Figure 5b) accommodated most of the sediments accumulating along the western margin of the horst, but by Sequence 2C and 2D and into Sequence 3, sediments were accumulating in the hanging-wall of Fault 9, while Fault 4 was to some degree uplifted in the footwall of Fault 9 as displacement across Fault 9 increased. This is highlighted in a comparison of the cross sections F-F' and G-G' (Figure 5) where the thickness variation of Sequence 2 across Fault 4 is seen to decrease significantly above 2C, while it increases significantly across Fault 9 from Sequence 2C to 3.

Discussion

The border fault system, unlike those to the north (Karonga basin, Mortimer et al., 2007) is not superimposed upon an underlying Ubendian fabric. The border fault nucleation and growth through fault tip propagation and linkage through breaching relay structures between overlapping segments (Trudgill and Cartwright, 1995) occurred in a manner anticipated for normal fault systems (Dawers and Anders, 1995; Trudgill and Cartwright, 1995; Gupta et

al., 1998; Cowie et al., 2000). This evolution leads to predictable sediment distribution with deposition progressively focussed toward the centre of the border fault array as it lengthens (McLeod et al., 2004) as is observed on the present day central basin (Figures 4 and 5). The Mbamba Fault initially played an important role in controlling sediment dispersal across the basin. Its location, directly opposite the central segment of the border fault system suggests that strain across the central part of the basin was accommodated on the Mbamba Fault until the central segment of the border fault system had linked and the full length established during Sequence 2. The Mbamba Fault is located directly opposite what is now the region of greatest sediment accumulation and lake depth on the MNF (and the entire basin).

The intra-basin region is dominated in the north and the centre by the presence of a horst that trends parallel to the MNF, and is offset across Fault 9. Very few faults exist between these larger displacement structures in the centre of the basin and the border fault, such that by the end of Sequence 1A strain was already localised into these regions, and the border faults had already accrued significant displacement. The early development of the horst region was of opposing half-graben bounded by faults up to 10 km in length and a few hundred meters of displacement separated across Fault 9 (and possibly other smaller NE-SW-trending structures) where their fault tips overlapped or converged. Each major fault (i.e., Fault 1 and 5) was antithetic to the dominant border fault; which during the early stage of the basin history included the Mbamba fault to the east. In a similar sense, the northern half of Fault 2 (later to become the eastern bounding fault of the horst) was

propagating with an opposing asymmetry to Fault 1. As the basin evolved, so the horsts established their length through the development of faults antithetic to these earlier faults. The pattern of intra-basin faulting for the majority of the structures striking slightly oblique to the MNF is consistent with modelled rift basins (Clifton et al., 2000; McClay et al., 2000; Corti et al., 2007) in regions where the extension direction is slightly oblique with respect to the existing structural framework. As these internal faults propagated along-strike, internal regions of the basin became compartmentalized into two areas west and east of the central horsts.

The flower cross-section geometry of Fault 9 indicates that it is active in a strike-slip sense, although the duration of fault activity cannot be ascertained. Its location between two converging intra basin faults (Faults 1 and 5) in the early stages of basin formation, give rise to a convergent transfer zone in which Fault 9 is the transfer fault (*e.g.,* Ebinger, 1989; Morley, 1990; Corti et al., 2007; Debapriya and Shankar, 2013) striking obliquely to the extension orientation. We suggest that Fault 9, and other similar striking faults within the basin were active from the earliest stages of basin evolution producing smaller intra-basin transfer zones, mirroring those larger-scale zones of accommodation and transfer between the Karonga and Nkhata Basin, and others along the rift. As extension within the basin continued, so the component of dip-slip along Fault 9 increased, such that it in turn became a significant feature affecting sediment distribution within the basin.

Basin summary and synthesis:

A summary of the basin evolution is presented in Figure 6, and constitutes the following steps: [1] Sequence 1A: Most of the major faults were established and the MNF was segmented with a significantly smaller segment to the south. The Mbamba Fault was similar in scale to the central segments of the border fault. In the centre of the basin, smaller intra-basin faults striking parallel to the border fault system formed a convergent transfer zone in the north separated by Fault 9, while to the south similar structures are observed. [2] Sequence 1B: the intra-basin horsts are well-defined along the basin axis, as faults antithetic to the existing structures in the centre of the basin form. Deposition is focussed adjacent to the MNF and to depocentres along the west margin of the horst in the north, and across the basin in the centre-south. [3] Sequence 2A to base 2C: the MNF formed a linked array through the breaching of relays as the north and central segments linked. The horsts in the central region were fully established along strike, separating the basin across west and east. Smaller, new faults develop adjacent to Fault 9 creating smaller compartments to the north and south as extension across the transfer continues. At the same time, the basin becomes asymmetric along its entire length; [4] Sequence 2C-3: the central 2 segments become fully linked with one depocentre, coupled with a marked reduction in the amount of sediment accommodated in the hanging-wall of the Mbamba Fault as strain became localised onto the MNF in the west. Fault 9 accumulated increasing amount of displacement, while Fault 4 became less important.

The role of the Karoo trend and structural inheritance:

To the east of the Malawi basin is the Karoo (Permo-Triassic) Ruhuhu graben; the northern margin of this system coincides with the rift-scale wide transfer zone between the north and central basins (Rosendahl 1987; Morley 1990). The southern boundary of the Ruhuhu graben also strikes parallel to and is along the fault trace of Fault 9 (Figures 1 and 4); and the trend of this continues to the location of the early basin high between depocentres adjacent to the central segment of the border fault system.

We suggest that the Ruhuhu graben, or an extension of its associated structures, controls the location and orientation of Fault 9 within the central basin. The orientation of such structures may have acted as early rupture barriers, and influencing the location of fault tips (Mbamba Fault) and segment boundaries (MNF central segments), which were subsequently overcome. Additional structures associated with the Ruhuhu graben probably also determine the location of other NE-SW striking faults within the basin. These existing structures coupled with the extension orientation are ideal for localising strike-slip or transfer faults. As previously noted, the geometry of Fault 9 separating Faults 1 and 5 is reminiscent of regional-scale opposing half-graben separated by accommodation zones localised onto existing structures (e.g., Versfelt and Rosendahl, 1989), but occurs here at the basin-scale. Not only, therefore, are existing earlier extensional structures important at the rift scale, they are important in determining the further differentiation and internal architecture of individual rift basins (Corti et al., 2007). To the south of the basin, Fault 10 follows a similar structural trend and coincides with the start of the wide transfer zone between the Nkhata and southern

basins. Thus existing pre-Cenozic structures have controlled the location of intra-basin transfer zones that become increasingly important as the amount of dip-slip across them accrues. This contrasts strongly with the asymmetric Karonga basin to the north, which does not experience the influence of underlying Karoo fabrics to the same effect, nor contains transfer faults within the basin (Mortimer et al., 2007).

Sediment distribution and hydrocarbon implications

This pattern of fault evolution has led to more complex sediment distribution and later dissections than might be anticipated. There are two main points of sediment entry into the Central basin: the Rukuru river (and delta) that enters the basin along the central border fault segment through the relay structure; and the Ruhuhu river which enters along the Ruhuhu Graben (Figure 7). During the early Sequences of deposition (Sequence 1A and B) sediments were relatively well distributed across the basin (Figure 4a-b); however in later sequences (from Sequence 2, Figures 4c-g) the east of the basin becomes increasingly comparatively starved, and in places would likely have been exposed during lake-level lowstand. This is especially pronounced by observing the distribution of sediment during Sequence 2B (Figure 4e) and Sequence 3 (Figure 4g). There is unlikely to have been significant transfer of coarse grained sediment from the western margin toward the east due to the presence of the linked horsts along the axis of the basin from Sequence 2A. Additionally, displacement across Fault 9 led to a reduction in the transport south along the eastern margin of the horst, and created a ponding effect to

the west of the horst, leading to a tongue of sediment being transported into the region between Fault 1 and 9 (Figure 4d-g).

During Sequence 2, as the oblique-slip extension across Fault 9 increased and Faults 1 and 5 separated further, new, smaller faults dissect the region immediately adjacent to Fault 9 and the earlier depocentres associated with the major intra-basin faults. This leads to a highly compartmentalized depocentres adjacent to the transfer fault.

Soreghan et al (1999) have well documented the distribution of sediments along the western part of the central basin. They record a channel network both through the relay zone (Rukwa River) and an additional channel from the Ruhuhu graben into the central part of the basin (Figure 7). Wells et al. (1995) and Soreghan et al (1999) show that coarse-grained material deposited dominantly in gravity driven flows accumulate on the relay ramp during highstands but otherwise are transported through canyons to the offshore area adjacent to the tips of the overlapping fault segment . The systems in the intra-basin region are confined by the western margin of the horst structures defined in our study. Similarly, a channel they document entering the basin from the north must flow around the propagating tip of the northern extent of the central horst system documented here. They observe that the coarsest material is ponded adjacent to the bounding and principal controlling structures as might be anticipated. This pattern of distribution for the latest stages of deposition is closely related to the present day fault configuration. Earlier deposition was better distributed to the east and along-axis before the

full linkage of the horst structures and significant displacement accumulation on or associated with Fault 9.

Implications for petroleum systems:

Intra-basin structures have been shown to exert an important influence on the evolution, sedimentary facies distribution and hydrocarbon trapping in rift basins (e.g. Bartholomew et al., 1993; Erratt et al, 1999; Whipp et al., 2014) and passive margin rift systems are dissected by cross cutting faults, in a similar geometry observed in Malawi (Paton et al., 2008, Tsikalas et al., 2008; Antobreh et al., 2009; Heine et al., 2013). Often these structures are not well defined as a consequence of poor quality data, wide spacing of available 2D lines, or a sub-salt setting. Understanding their role is of particular importance in frontier areas where 2D data is utilised. Our findings in the Malawi Rift can be applied to rift basin exploration elsewhere, in particular in highlighting the importance of underlying structures in controlling the initial intra-basin fault behaviour and predicting their effect on sediment transport and basin architecture (Figure 8).

The scenario outlined here, in which there is a fabric cross-cutting the main rift geometry allows us to make some key predictions: the principal intra-basin faults are approximately co-linear and grow through time. This results in relatively linear axial sand fairways controlled by intra-basin faults. The cross-cutting faults are active as transfer faults likely to cause localised deflection of the fairway and result in a oblique stacking pattern of channel systems at the step-over zone. As dip-slip displacement accumulates on the developing

structure, so sediment pathways are disrupted and sediment ponding occurs, while dissection of existing depocentres continues as the lateral offset along the cross-cutting structures increases.

This has two implications: (1) fairway distribution may be controlled less by the main intra-basin faults, while local depocentres at accommodation zones may occur; and (2) previously continuous sand fairways that were migration pathways for charge from the down-dip kitchen to up-dip flanks, become highly compartmentalized while juxtapositions across the structures change significantly.

Acknowledgements

Funding for EM was provided by DFG grant STR 373/15-1 and by the Basin Structure Group at the University of Leeds. Support for the field acquisition of single-channel seismic reflection data was provided by the Industrial Associates of the Lacustrine Rift Basin Research Program at Syracuse University, C. A. Scholz, Principal Investigator. Multichannel seismic reflection data was acquired under the auspices of Project PROBE at Duke University, under the direction of B. R. Rosendahl.

References

Antobreh, A.A; Faleide, J.I ; Tsikalas, F. ; Planke, S., 2009, Rift-shear architecture and tectonic development of the Ghana margin deduced from multichannel seismic reflection and potential field data: Marine and Petroleum Geology v.26, p.345-368.

Bartholomew, I. D, Peters, J. M. Powell, C. M., 1993, Regional structural evolution of the North Sea: oblique slip and the reactivation of basement lineaments: Petroleum Geology Conference series, v.4, p.1109-1122, doi:10.1144/0041109.

Biggs, J., Nissen., E., Craig, T., Jackson, J., Robinson, D.P., 2010, Breaking up the hanging wall of a rift border fault: the 2009 Karonga earthquakes, Malawi. Geophysical Research Letters, v.37:L11305.

Clifton, A.E., Schlische, R.W., Withjack, M.O., and Ackermann, R.V**.,** 2000, Influence of rift obliquity on fault-population systematics: results of experimental clay models: Journal of Structural Geology, v.22, p.1491-1509.

Contreras, J., Anders, M. H. & Scholz, C. H., 2000, Growth of a normal fault system: observations from the Lake Malawi basin of the east African rift: Journal of Structural Geology, v.22, p.159-168.

Corti, G., van Wijk, J., Cloetingh, S., Morley, C.K., 2007, Tectonic inheritance and continental rift architecture: Numerical and analogue models of the East African Rift system: Tectonics, v. 26, n.6, doi:10.1029/2006TC002086.

Cowie, P.A., Vanneste, C., and Sormette, D., 1993, Statistical physical model for the spatio-temporal evolution of fault: Journal of Geophysical Research, v.98, p. 21809-21821.

Cowie, P. A., Gupta, S., and Dawers, N.H., 2000, Implications of fault array evolution for syn-rift depocentre development: insights from a numerical fault-growth model: Basin Research, v. 12, p. 241-261.

Dawers, N.H., and Anders, M.H., 1995, Displacement-length scaling and fault linkage: Journal of structural Geology, v.17, p.607-614.

Delvaux, D.,and Barth, A., 2010, African stress Pattern from formal inversion of focal mechanism data. Implications for rifting dynamics. Tectonophysics, v.482, p. 105-128.

Delvaux, D., Levi., K., Kajara., R. & Sarota, J., 1992, Cenozoic paleostress and kinematic evolution of the Rukwa-north Malawi rift valley (EARs): Bull. Cent. Rech. Explor. –prod Elf Acquitaine, v. 16, p. 383-406.

Ebinger, C. J., Deino, A. L., Tesha, A. L., Becker, T: & Ring, U., 1993, Tectonic controls on rift basin morphology: evolution of the Northern Malawi (Nyasa) rift: Journal of Geophysical Research, v.98**,** p.17821-17836.

Ebinger, C. J., Rosendahl, B. R. and Reynolds, D. J., 1987, Tectonic model of the Malawi rift, Africa: Tectonophysics, v.141**,** p.215-235.

Ebinger, C. J., Crow, M. J., Rosendahl, B. R., Livingstone, D.A. and Le Fournier, J., 1984, Structural evolution of Lake Malawi, Africa: Nature*,* v.308**,** p.627-629.

Errat, D., Thomas, G.M., and Wall, G.R.T., 1999, Regional syntheses, tectono-stratigraphic analyses and structural studies: The evolution of the Central North Sea Rift : Petroleum Geology Conference series, v.5, p.63-82, doi:10.1144/0050063

Flannery, J.W. & Rosendahl, B.R., 1990, The seismic stratigraphy of Lake Malawi: implications for interpreting geological processes in lacustrine rifts: Journal of African Earth Science, v.10, p.519-548.

Gupta, S., Cowie, P.A., Dawers, N.H, & Underhill, J.R, 1998, A mechanism to explain rift-basin subsidence and stratigraphic patterns through fault array evolution: Geology*,* v. 26, p. 595-598.

Heine, C., Zoethout, J., and Muller, R. D., 2013, Kinematics of the South Atlantic rift, Solid Earth, v.4, p.215–253

Hubbard, R.J., Pape, J. & Roberts, D.G., 1985a, Depositional sequence mapping as a technique to establish tectonic and stratigraphic framework and evaluate hydrocarbon potential on a passive continental margin, in Beerg, O.R. and Wooverton, D.G ed, Seismic stratigraphy II: AAPG Memoir 29, p.79-92.

Hubbard, R.J., Pape, J. & Roberts, D.G (1985b), Depositional sequence mapping as a technique to establish tectonic and stratigraphic framework and evaluate hydrocarbon potential on a passive continental margin, in, Beerg, O.R. and Wooverton, D.G ed, Seismic stratigraphy II: AAPG Memoir 29, p 93-116.

Mitchum, R.M. Jr, Vail, P.R. and Sangree, J.B., 1977, Seismic stratigraphy and global changes of sea-level part 6: seismic stratigraphic interpretation procedure, in, Payton, C.E. ed, Seismic stratigraphy- applications to hydrocarbon exploration: APPG Memoir, 26, p 117-134.

McClay, K.R., Dooley, T., Whitehouse, P. & Mills, M., 2002, 4-D evolution of rift systems: Insights from scale physical models: Bulletin of the American Association of Petroleum Geologists, v. 86, p. 935-959.

McLeod, A.E., Dawers, N.H., & Underhill, J.R., 2000, The propagation and linkage of normal faults: insights from the Strathspey-Brent-Statfjord fault array, northern North Sea: Basin Research, v.12, p.263-284.

Morley, C.K., 1995, Developments in the structural geology of rifts over the last decade and their impact on hydrocarbon exploration, in, Lambaise, J.J. ed., Hydrocarbon habitat in rift basins: Geological Society Special Publication, v.80, p. 1-32.

Morley, C.K., Nelson, R.A., Patton, T.L., and Munn, S.G., 1990, Transfer Zones in the East African Rift System and Their Relevance to Hydrocarbon Exploration in Rifts (1): AAPG Bulletin, v. 74, n. 8, p.1234-1253

Mortimer, E.J., Paton, D.A., Scholz, C.A., Strecker, M.R., and Blisniuk, P 2007, Orthogonal to oblique rifting: effect of rift basin orientation in the evolution of the North Basin, Malawi Rift, East Africa: Basin Research, v.19, n.3, p.393-407, DOI: 10.1111/j.1365-2117.2007.00332.x

Mortimer, E.; Foeken, J.; Strecker, M.; Stuart, F., 2006, Evolution of a Young Rift Border-Fault System Constrained by Low Temperature (U-Th/He) Thermochronometry: North Basin, Malawi Rift, East Africa, abstract , AGU Fall Meeting.

Paton, D.A., 2006, Influence of crustal heterogeneity on normal fault dimensions and evolution: southern South Africa extensional system: Journal of Structural Geology, v.28, p.868-886.

Paton, D.A., van der Spuy, D, di Primio R., Horsfield, B., 2008, Tectonically induced adjustment of passive-margin accommodation space; influence on the hydrocarbon potential of the Orange Basin, South Africa: AAPG Bulletin, AAPG Bulletin, v.92, p.589–609.

Prosser, S., 1993, Rift-related linked depositional systems and their seismic expression, in, Williams, G.D. and Dobb, A. ed., Tectonics and seismic sequence stratigraphy: Special publication of the Geological Society, London, v.71, p.35-66.

Reynolds, D.J., and Rosendahl, B.R., 1984, Tectonic expressions of continental rifting: EOS, Trans AGU, v.65 , p.1116.

Reinecker, J., Heidbach, O., Tingay, M., Sperner, B. & Müller, B., 2005, The release 2005 of the World Stress Map (available online at www.world-stress-map.org)

Ring, U., Betzler, C., and Delvaux, D, 1992, Normal vs. Strike-slip faulting during rift development in East Africa: the Malawi rift: Geology, v.20, p.1015-1018.

Ring, U., Betzler, C., and Delvaux., D, 1992, Normal vs. Strike-slip faulting during rift development in East Africa: the Malawi rift: Geology, v.20, p.1015-1018.

Roberts, E.M., Stevens, N.J, O'Connor, P.M., Dirks P.H.G.M., Gottfried, W.C., Clyde, W.C., Armstrong, R.A., Kemp, A.I.S., Hemming, S., 2012, Initiation of the western branch of the East African Rift coeval with the eastern branch: Nature, v.5, p.289-294.

Rosendahl, B.R., 1987, Architecture of continental rifts with special reference to East Africa: Annual Review of Earth Planetary Science, v.15, p.445-503.

Scott, D. L., Etheridge, M.A., and Rosendahl, B.R., 1992, Oblique-slip deformation in extensional terrains: a case study of the lakes Tanganyika and Malawi rift zones: Tectonics, v.11, p.998-1009.

Scholz, C. A., 1995, Seismic stratigraphy of an accommodation-zone margin rift-lake delta, Lake Malawi, Africa, in, Lambiase, J.J, Hydrocarbon Habitat in Rift Basins: Geological Society Special Publication, v.80, p.183-195.

Scholz, C.A.,1989, Project PROBE geophysical atlas series, Duke University, Durham, N.Carolina.

Schlische R.W. and Anders, M.H., 1996, Stratigraphic effects and tectonic implications of the growth of normal faults and extensional basins: Geological Society of America Special Paper, v.303, p.183-203.

Soreghan, M.J., Scholz, C.A., and Wells, J.T., Coarse-grained deep-water sedimentation along a border fault margin of Lake Malawi, Africa: seismic stratigraphic analysis. *Journal of Sedimentary Research,* **69,** 1999, 832-846

Trudgill, B. and Cartwright, J., 1994, Relay-ramp forms and normal-fault linkages, Canyonlands National Pak, Utah: Bulletin of the Geological Society of America, v.106, p.1143-1157.

F. Tsikalas, J.I. Faleide, and N.J. Kusznir, 2008, Along-strike variations in rifted margin crustal architecture and lithosphere thinning between northern Vøring and Lofoten margin segments off mid-Norway: Tectonophysics, v.458, p.68-81.

Versfelt, J. and Rosendahl, B.R., 1989, Relationships between pre-rift structure and rift architecture in Lakes Tanganyika and Malawi, East Africa: Nature, v.337, p.354-357.

Wells, J.T., Scholz, C.A., and Soreghan, M.J., Processes of sedimentation on a lacustrine border-fault margin: interpretation of cores from Lake Malawi, East Africa. *Journal of Sedimentary Research,* **69**, 1999, 816-831.

Wheeler, W. H. and Rosendahl, B.R., 1994, Geometry of the Livingstone Mountains Border-fault, Nyasa (Malawi) Rift, East Africa: Tectonics, v.13, p. 303-312.

Wheeler, W.H., and Karson, J.A., 1989, Structure and kinematics of the Livingstone mountain border-fault zone, Nyasa (Malawi) rift, south-western Tanzania: Journal of African Earth Sciences, v. 8, p.393-414.

Withjack, M.O. and Jamison, W.R., 1986, Deformation produced by oblique rifting: Tectoniphysics, v.126, p.99-124.

Whipp, P.S., Jackson, C. A-L., Gawthorpe, R. L., Dreyer, T., and Quinn, D., 2014, Normal fault array evolution above a reactivated rift fabric; a subsurface example from the northern Horda Platform, Norwegian North Sea: Basin Research, v.26, p.523-549.

FIGURE CAPTIONS

Figure 1: a) The location the Malawi Rift, the southernmost portion of the western branch of the East African Rift System; (b) Simplified geology of the northern Malawi Rift region extending to the Rukwa Rift ; with the study area outlined in the black box.

Figure 2 a) Two Way Travel Time (ms TWT) map to lake bed within the Nkhata Basin, seismic reflection data of the PROBE study (1989) shown in solid dark grey lines, shallow seismic reflection data in solid pale grey lines. Principal structures identified within the seismic reflection data are indicated in black with ticks on the downthrown side; b) Isopach (thickness TWT) map of the sedimentary fill of the Central Basin with principal structures shown. The points of entry of the principal sediment sources (the South Rukuru and the Ruhuhu Rivers) are indicated.

Figure 3: Cross-sections through the Nkhata Basin showing the principle structures from north to south. In the north, close to the transfer to the Karonga Basin, the Nkhata Basin is strongly asymmetrical thickening to the west into the north segment of the Mlowe-Nkhata Fault (MNF) and shoaling to the east. This asymmetry remains, but is less pronounced as we move to the south in section B-B' but with the addition of the Northern horst dividing the

basin. In the centre of the basin adjacent to the central segment of the MNF the basin the geometry is more symmetrical with a central horst and similar depth to basement on both the east and west margins, in particular adjacent to the Mbamba Fault in Section C-C'. Sedimentation across the horsts is asymmetric, with the west (MNF side) accommodating more sediment. Further south, there is a subtle high adjacent to the MNF in section D-D' corresponding to the region of overlap between the central and southern segments. In the far south of the basin, the geometry is again of a horst-graben with fault 6, west-dipping and bounding the southern horst accommodating a similar amount of displacement as the southern segment of the east-dipping MNF.

Figure 4: TWT Isopach maps of the Central Basin for each depositional sequence. PROBE data has been used for Sequence 1 (A and B). Shallow seismic reflection data were used for Sequences 2B,C and D whereas the total Sequence 2 (A-D) is the thickness of the entire Sequence present within the PROBE data (base Sequence 2 not present in the shallow). Sequence 3 is from the shallow seismic data (where present) supplemented by the PROBE data. See inset for outline of PROBE and shallow data coverage; and for fault numbers as discussed on the figure and in text. These maps show the migration of depocentres through time adjacent to the MNF and other faults. The MNF initially comprised 4 fault segments; the central two linking to form a single fault segment. Fault 9 is discussed in detail in the text, but has an important role in partitioning the basin; initially positioned along-trend from the structural high separating depocentres on the central MNF segment, and in ponding sediment in its hanging-wall (north) preventing sediment transport to the south and east of the basin. Faulting adjacent to fault 9 increases in complexity throughout Sequence 2, and in Sequence 3, folding occurs adjacent to the central MNF. These maps highlight the small-scale intra-basin partitioning

Figure 5: These sections, which most closely relate to PROBE section C-C' (see Figure 2), show the more detailed fault architecture associated with Fault 9. (top) F-F' cross-section through Fault 9 in the centre of the basin, showing the geometry of the fault and accommodation in its hanging-wall, in particular during the later stages of Sequence 2. (bottom) G-G' cross-section west-east across the basin through Fault 4 that connects to Fault 9 just to the north of this section.
Comparing these two sections highlights the similar structural style between them. It also shows the present day structural high associated with Fault 9 and adjacent faults that is important in sediment dispersal, particularly during lake-level fluctuations, and in influencing the distribution of sequences 2D and 3. Fault 9 accommodates more sediment in Sequences 2C-3 while Fault 4 was more important early in Sequence 2: from 2A to the base of 2B.

Figure 6: The proposed development of the Central Basin. Faults are numbered where referred to in the text and are shaded with dark grey on their fault scarps. Depocentres are shaded, deep brown representing the thickest region of sediment accumulation within the sequence.

Figure 7: Present day fault sediment dispersal within the northern part of the Central basin (after Soreghan et al., 1999 solid channels; and inferred, dashed channels) and the influence of the intra-basin structures from this study. The relay structure on the border fault system is important for sediment dispersal into the central segment, and in fans along the north segment. In the centre of the basin, sediments are transported along strike parallel to the horst structure and are ponded adjacent to fault 9. This is a region with abundant small-scale faulting. Very little sediment enters to the east of the central horst.

Figure 8: The influence of cross cutting structures within the rift basin on sand fairway distribution. Importantly for the EARS charge and migration occurs into the present day and will be most affected by the present day configuration, while fairway and reservoir distribution will have been determined by the primary basin structures. Initially (1) the transfer fault has little displacement, adjacent faults have individual depocentres controlling early syn-rift sedimentation and sediment pathways exist along-axis of the basin. (2) as the transfer fault offset continues, displacement along the structure begins to restrict sediment pathways, while depocentres along the connecting normal faults enlarge until (3) displacement within the hanging-wall of the transfer fault is significant, leading to ponding of sediment between the rift faults and transfer fault. This will become more pronounced during periods of lake-level lowstand (as commonly experienced within EARS lakes). The hydrocarbon consequence of this is twofold: Firstly, the sand fairway becomes segmented, with an up-dip charge this would result in either reservoir compartmentalization or at least baffling. Secondly, faults with the largest present day throw may not have been present during deposition of syn-rift sand, therefore their location may be misleading.

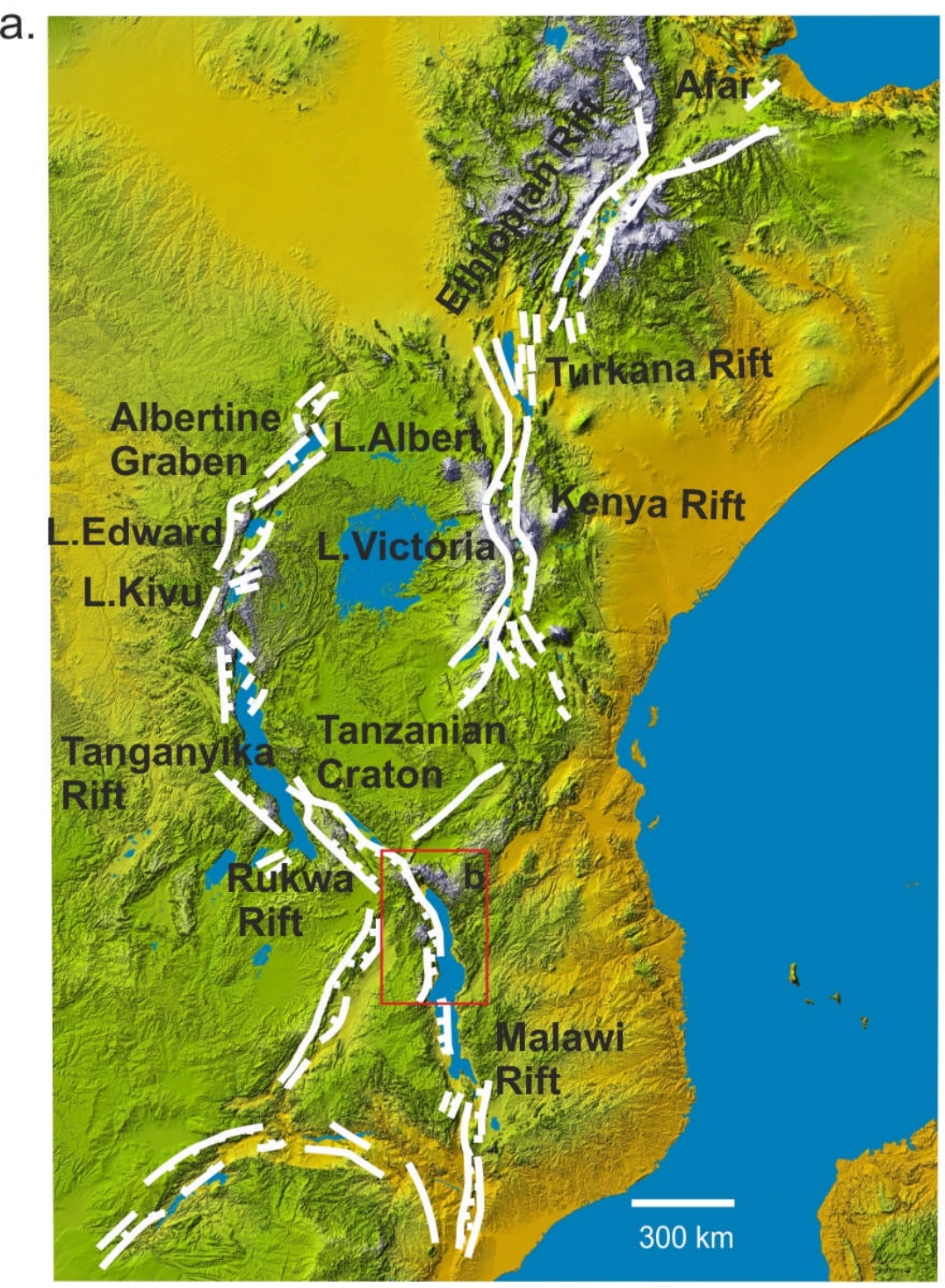
a.
Afar
Ethiopian Rift
Turkana Rift
Albertine Graben
L.Albert
Kenya Rift
L.Edward
L.Victoria
L.Kivu
Tanganyika Rift
Tanzanian Craton
Rukwa Rift
b
Malawi Rift
300 km

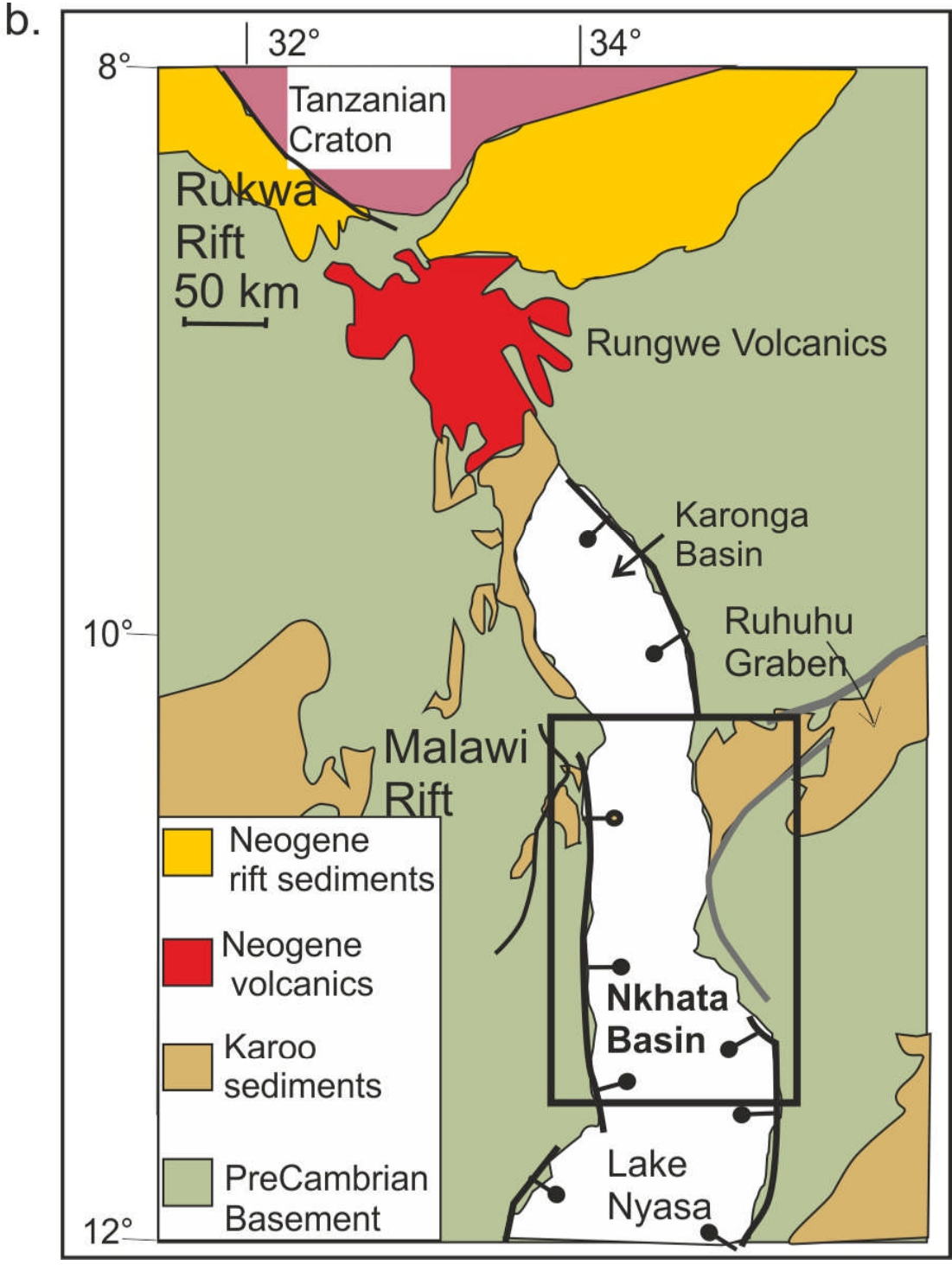
b.
32°
34°
8°
10°
12°
Tanzanian Craton
Rukwa Rift
50 km
Rungwe Volcanics
Karonga Basin
Ruhuhu Graben
Malawi Rift
Nkhata Basin
Lake Nyasa
Neogene rift sediments
Neogene volcanics
Karoo sediments
PreCambrian Basement

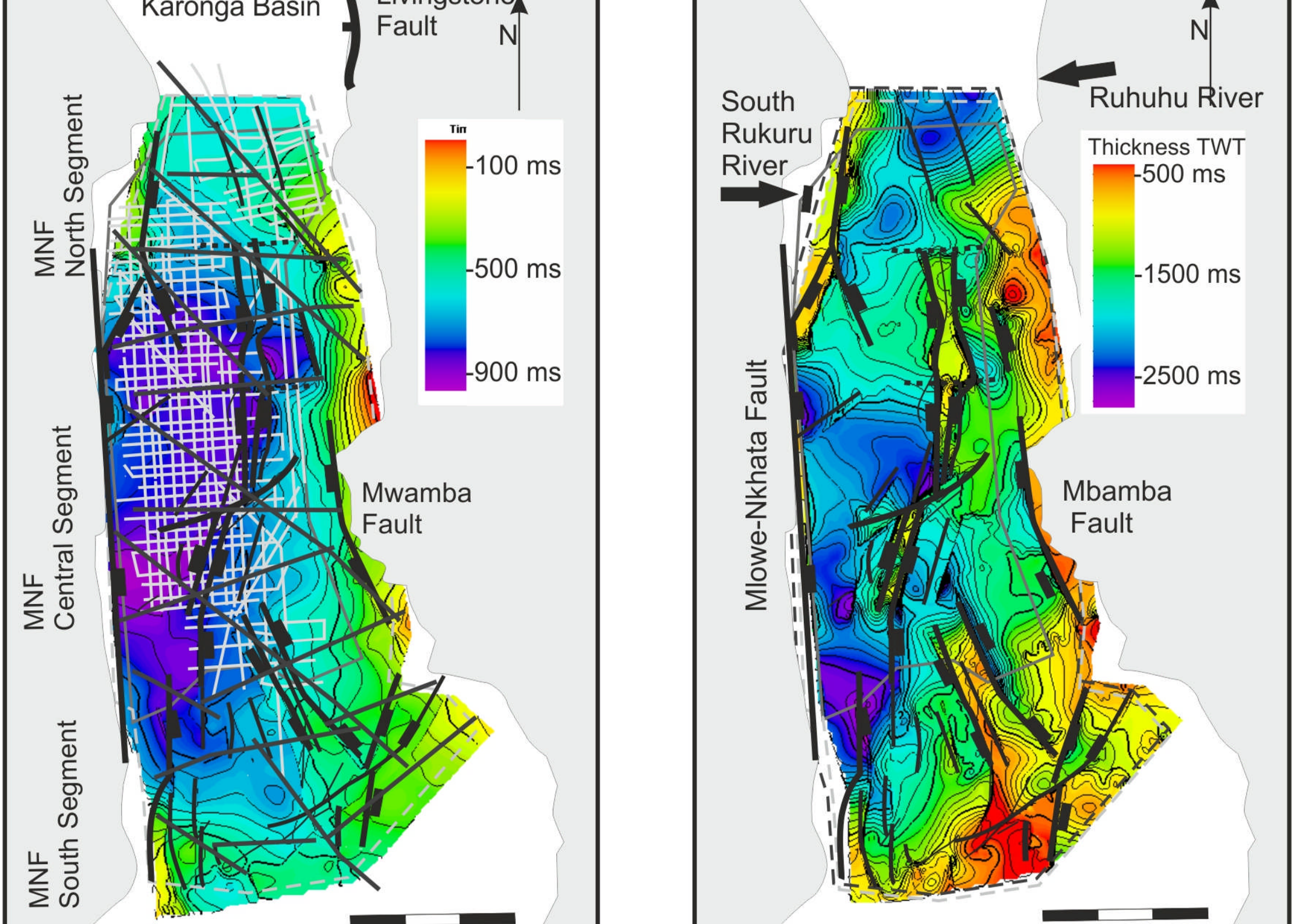
Karonga Basin
Livingstone
Fault
N
MNF
North Segment
MNF
Central Segment
MNF
South Segment
Mwamba
Fault
-100 ms
-500 ms
-900 ms
South
Rukuru
River
Ruhuhu River
N
Thickness TWT
-500 ms
-1500 ms
-2500 ms
Mlowe-Nkhata Fault
Mbamba
Fault

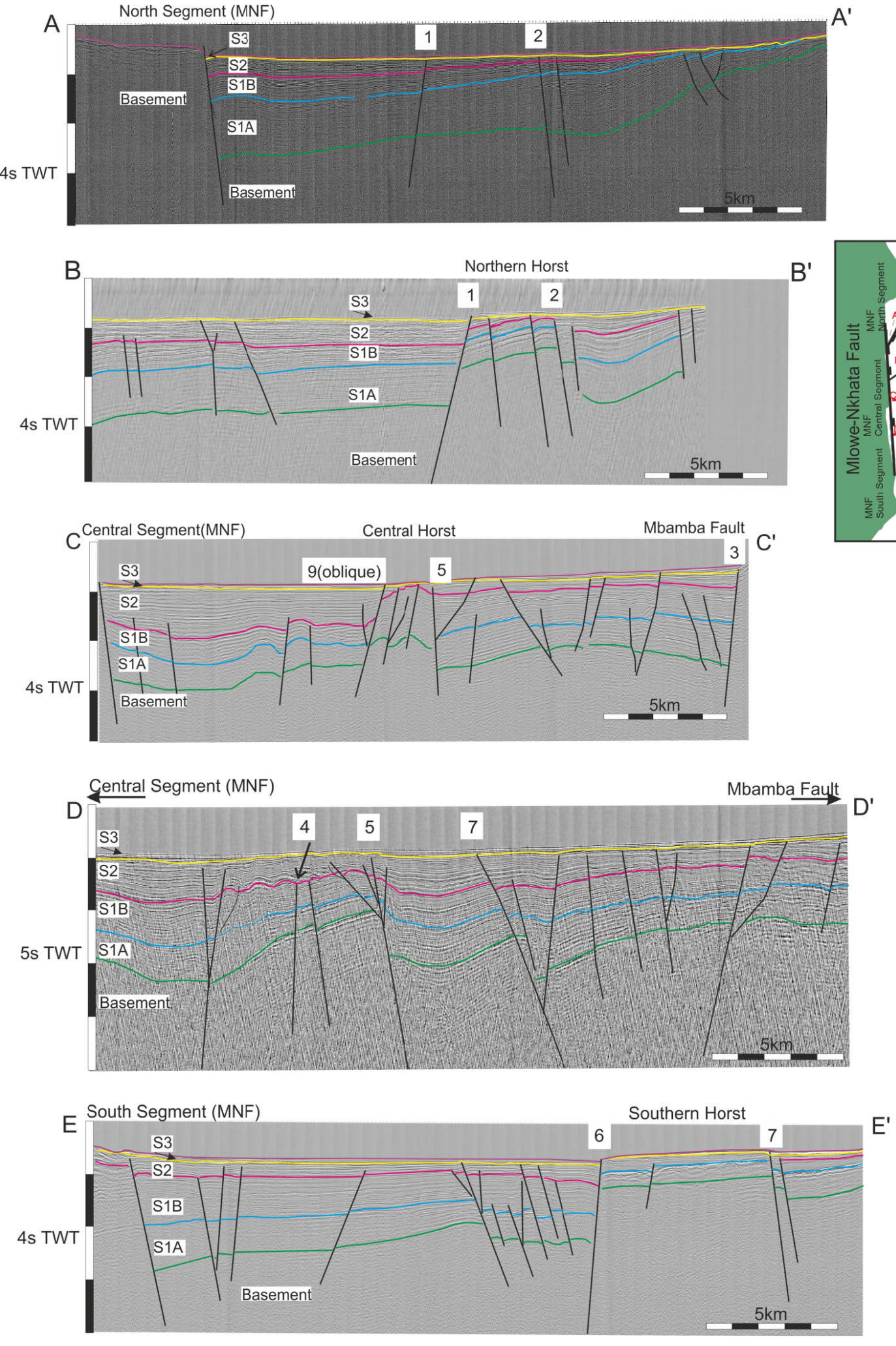
A
North Segment (MNF)
A'
S3
S2
S1B
S1A
Basement
Basement
1
2
4s TWT
5km
B
Northern Horst
B'
S3
S2
S1B
S1A
Basement
1
2
4s TWT
5km
C
Central Segment(MNF)
Central Horst
Mbamba Fault
C'
S3
S2
S1B
S1A
Basement
9(oblique)
5
3
4s TWT
5km
D
Central Segment (MNF)
Mbamba Fault
D'
S3
S2
S1B
S1A
Basement
4
5
7
5s TWT
5km
E
South Segment (MNF)
Southern Horst
E'
S3
S2
S1B
S1A
Basement
6
7
4s TWT
5km
30 km
N
Mlowe-Nkhata Fault
MNF
North Segment
MNF
Central Segment
MNF
South Segment
Mwamba
Fault "3"

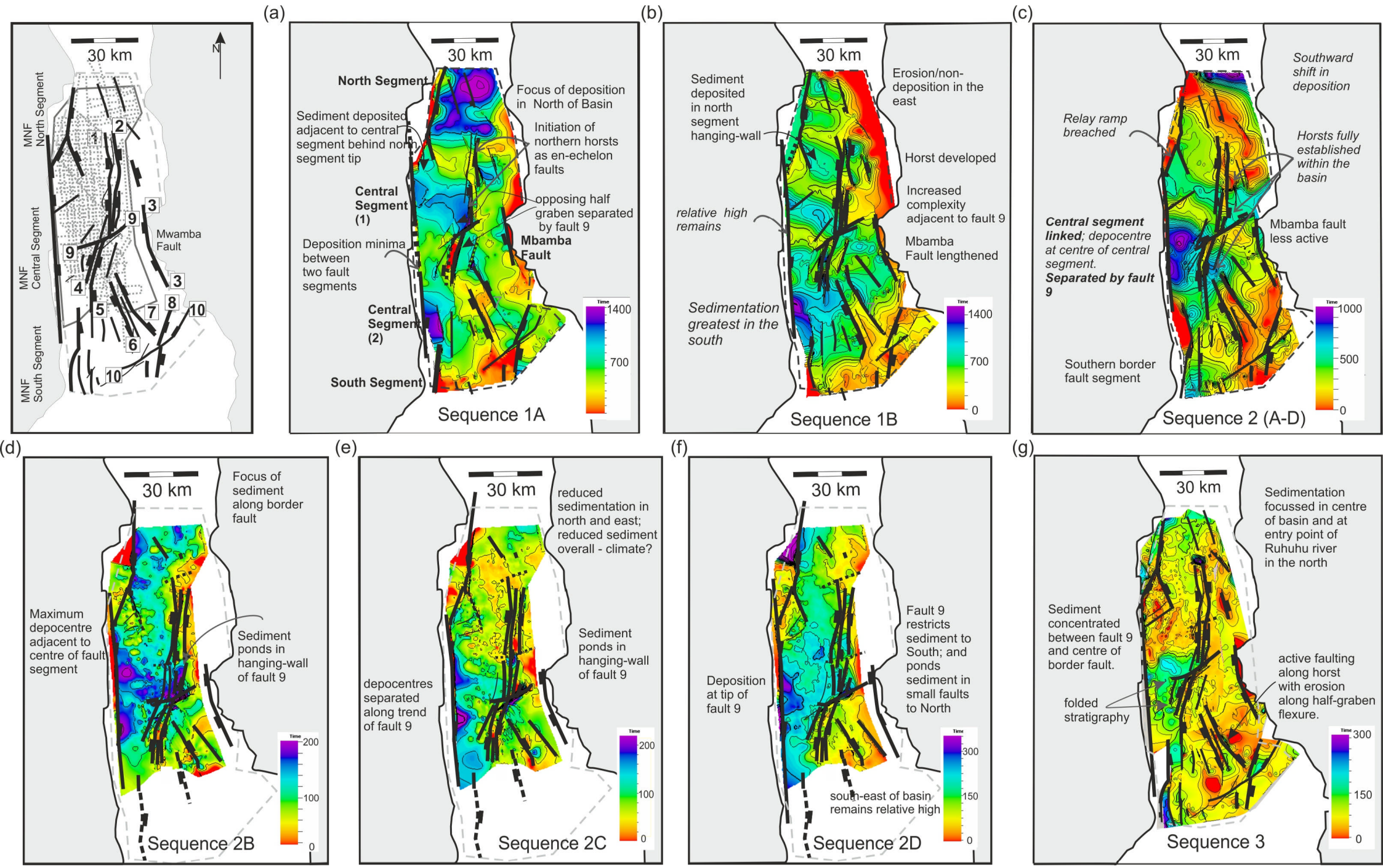
30 km
N
MNF North Segment
MNF Central Segment
MNF South Segment
Mwamba Fault
(a)
North Segment
Sediment deposited adjacent to central segment behind north segment tip
Focus of deposition in North of Basin
Initiation of northern horsts as en-echelon faults
Central Segment (1)
opposing half graben separated by fault 9
Mbamba Fault
Deposition minima between two fault segments
Central Segment (2)
South Segment
Time
1400
700
Sequence 1A
(b)
Sediment deposited in north segment hanging-wall
Erosion/non-deposition in the east
Horst developed
Increased complexity adjacent to fault 9
relative high remains
Mbamba Fault lengthened
Sedimentation greatest in the south
1400
700
0
Sequence 1B
(c)
Southward shift in deposition
Relay ramp breached
Horsts fully established within the basin
Central segment linked; depocentre at centre of central segment.
Separated by fault 9
Mbamba fault less active
Southern border fault segment
1000
500
0
Sequence 2 (A-D)
(d)
Focus of sediment along border fault
Maximum depocentre adjacent to centre of fault segment
Sediment ponds in hanging-wall of fault 9
200
100
0
Sequence 2B
(e)
reduced sedimentation in north and east; reduced sediment overall - climate?
depocentres separated along trend of fault 9
Sediment ponds in hanging-wall of fault 9
200
100
0
Sequence 2C
(f)
Deposition at tip of fault 9
Fault 9 restricts sediment to South; and ponds sediment in small faults to North
south-east of basin remains relative high
300
150
0
Sequence 2D
(g)
Sedimentation focussed in centre of basin and at entry point of Ruhuhu river in the north
Sediment concentrated between fault 9 and centre of border fault.
active faulting along horst with erosion along half-graben flexure.
folded stratigraphy
300
150
0
Sequence 3

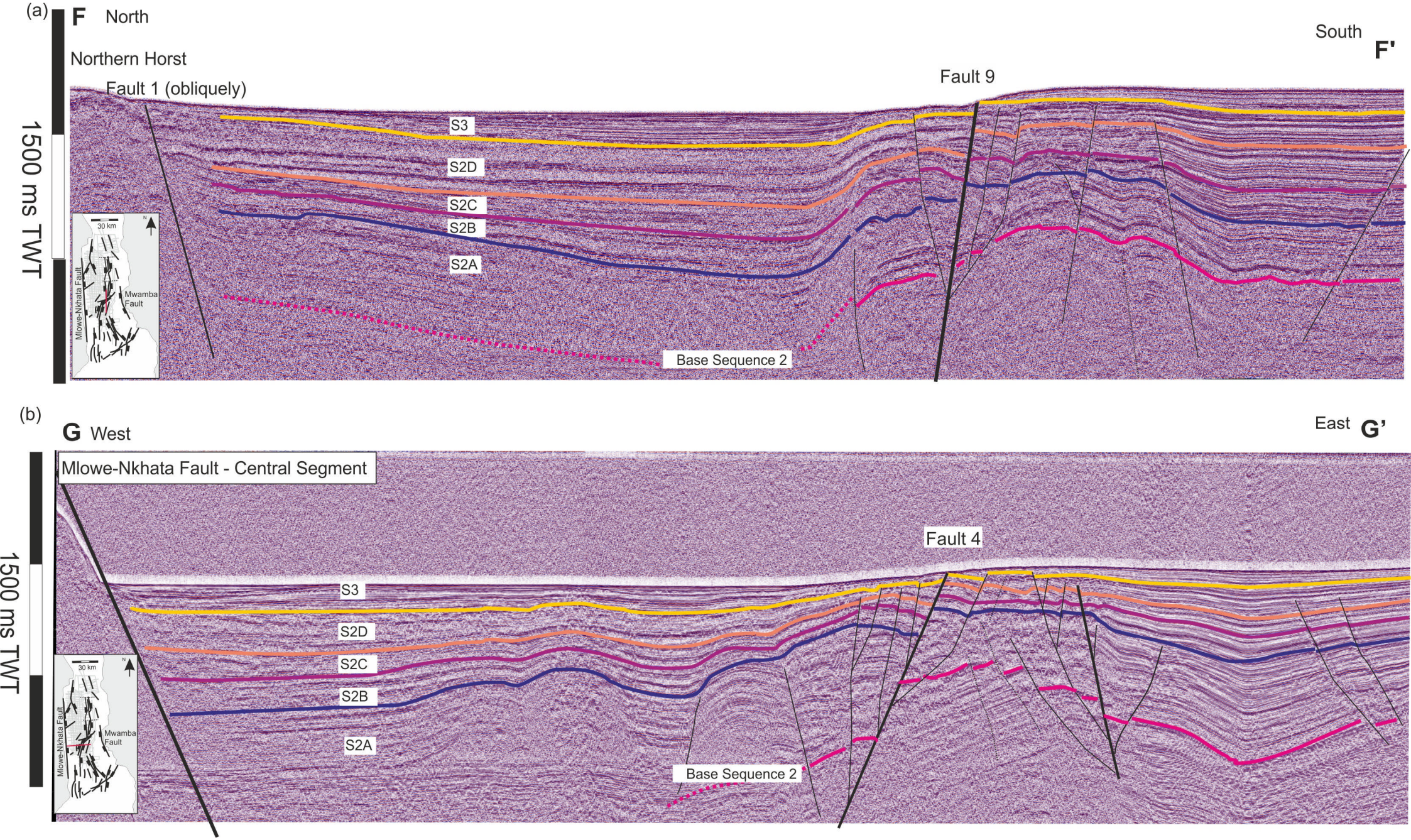
(a)
F
North
South
F'
Northern Horst
Fault 1 (obliquely)
Fault 9
1500 ms TWT
S3
S2D
S2C
S2B
S2A
Base Sequence 2
30 km
N
Mlowe-Nkhata Fault
Mwamba Fault
(b)
G
West
East
G'
Mlowe-Nkhata Fault - Central Segment
Fault 4
1500 ms TWT
S3
S2D
S2C
S2B
S2A
Base Sequence 2
30 km
N
Mlowe-Nkhata Fault
Mwamba Fault

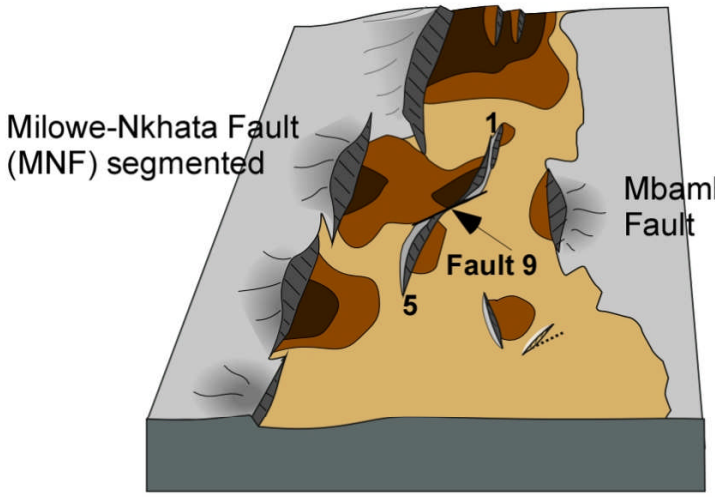

SEQUENCE 1A

Individual fault segments along the border fault; opposing half graben (bordered by Fault 5 and 1) across the center of the basin separated by Fault 9. Mbamba Fault active.

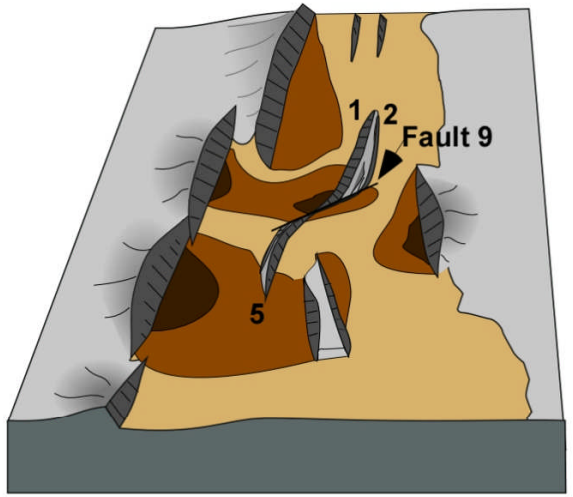

SEQUENCE 1B

Border fault segments develop and overlap. Horsts develop as displacement along fault 9 increases. Fault 4 and Fault 2 become more important.

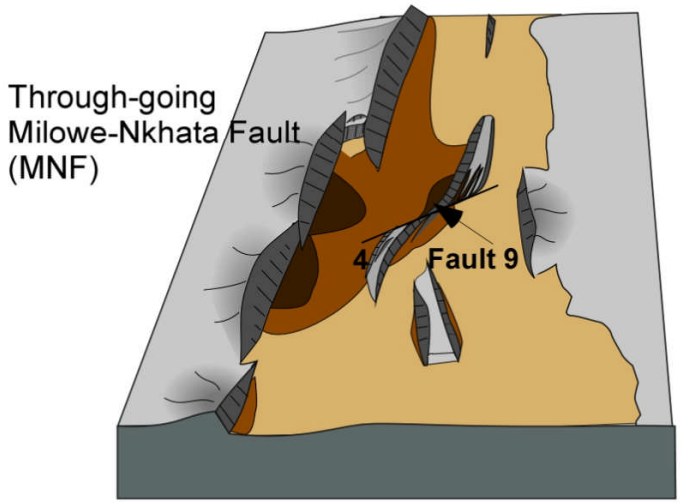

SEQUENCE 2A and 2B

Relay between the north and central segment of the MNF is developed. Central fault segments overlap. In the basin, faulting complexity adjacent to Fault 9 increases as displacement continues, displacement along Fault 9 leads to high in the south east and lack of sedimentation in south east. Fault 4 active in controlling sediment. Dissection of basin adjacent to Fault 9 - small depocenters can form in high-stand conditions.

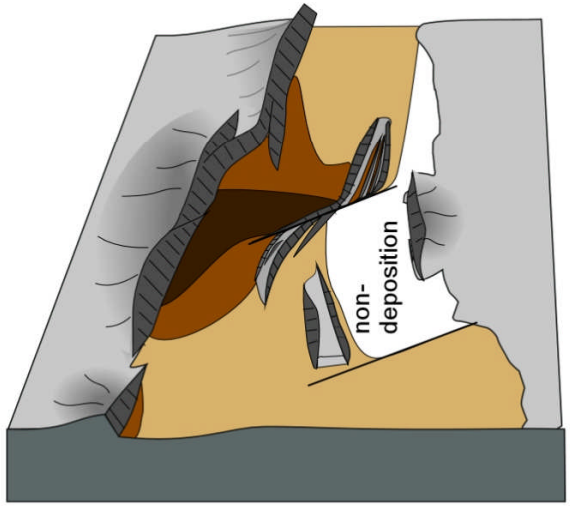

SEQUENCE 2C, D and 3

Central fault segments completely linked and one depocenter adjacent to them. Displacement *across* Fault 9 increases, leading to one larger depocenter between faults 1 and 9 while activity on Fault 4 reduces. Mbamba fault less important as strain is localised onto the MNF.

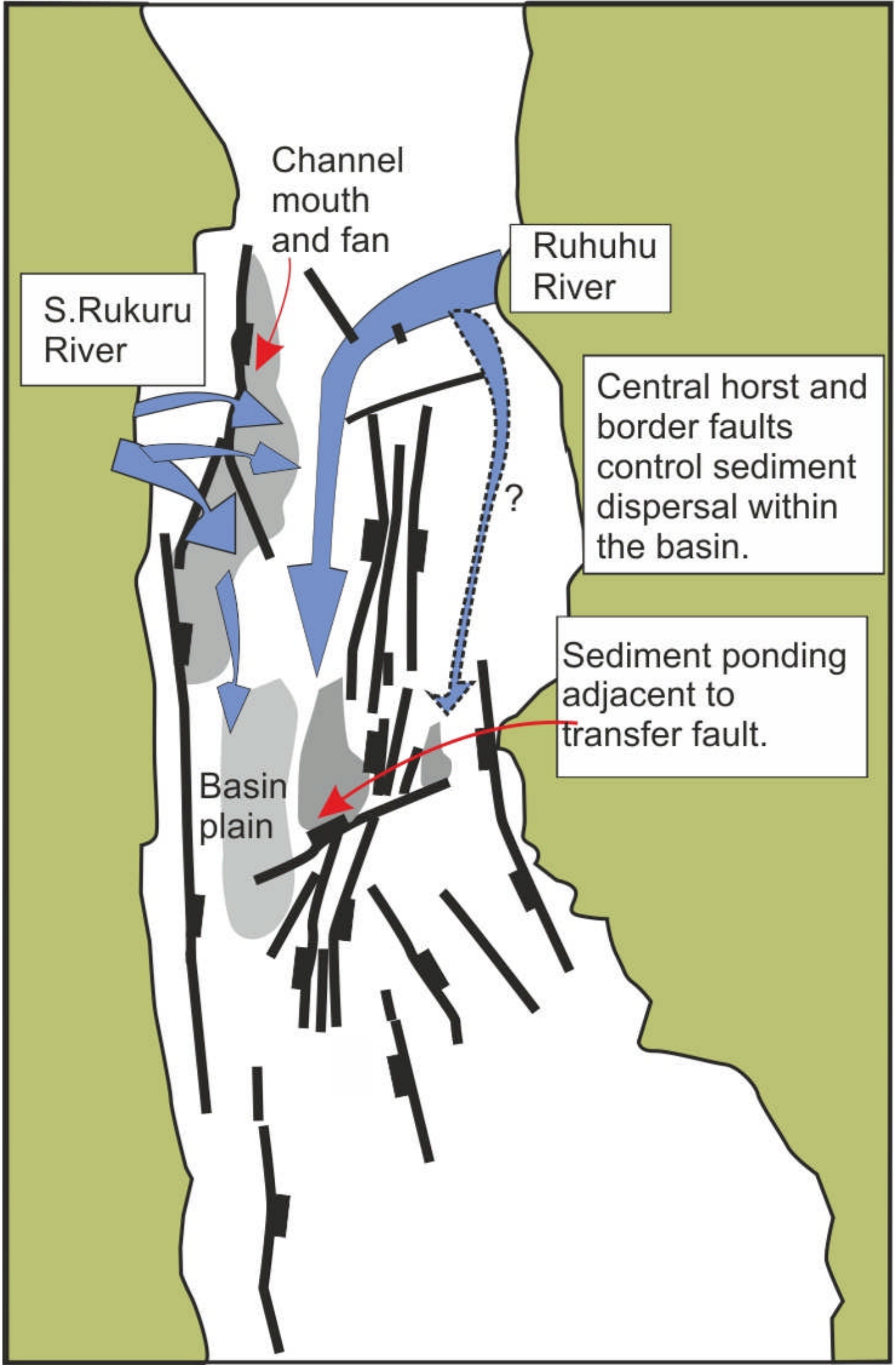
Channel mouth and fan
Ruhuhu River
S.Rukuru River
Central horst and border faults control sediment dispersal within the basin.
?
Sediment ponding adjacent to transfer fault.
Basin plain

Pre-existing fabric localises cross-cutting strike-slip deformation

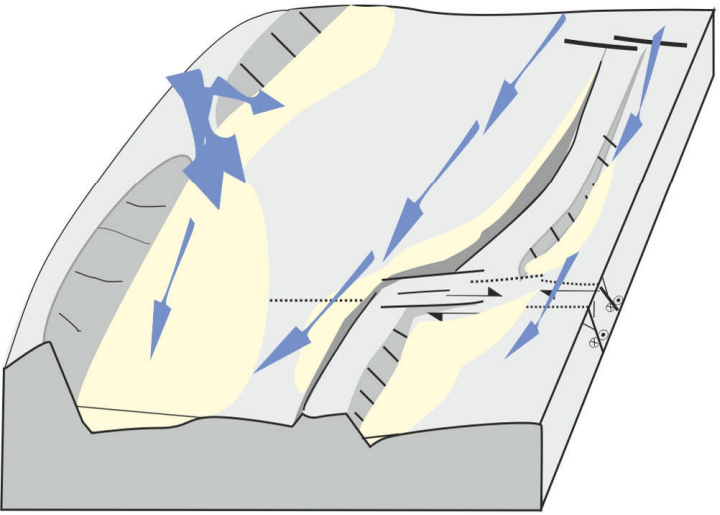

Cross-cutting faults result in lateral offset in sand-fairways although may be locally deformed with short wavelength folding and inversion structures

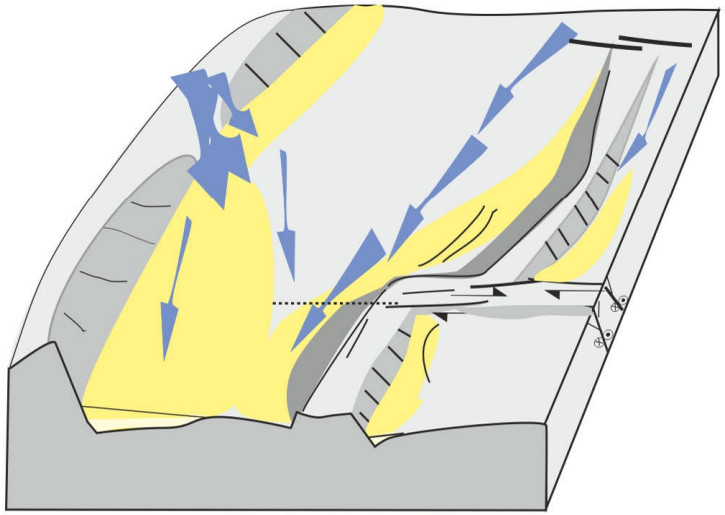

Location of sand fairways are controlled by intra-basin and basin bounding faults.